Distinguishing faults from flooding surfaces on spectral gamma-ray logs

A. Ruffell, J. M. McKinley, and R. Evans

ABSTRACT

Elevated gamma-ray emission from discrete beds in sedimentary deposits may conventionally be interpreted as representing flooding surfaces or transgressive beds. Potassium (K), uranium (U), or (less commonly) thorium (Th) concentrations in outcrop or borehole successions cause such elevated gamma-ray emission and may be linked to the presence of specific mineral hosts. Furthermore, specific Th/K and Th/U ratios occur at correlated stratigraphic surfaces and form part of a pattern that reflects a sequence-stratigraphic hierarchy. Spectral gamma-ray logs from uncored boreholes or weathered cliffsides and acquired without full petrographic descriptions can intersect low-angle faults such as thrusts. Our study demonstrates that bedding-parallel faults can be mistaken for flooding surfaces. We document the spectral gamma-ray response through a range of visually obvious and cryptic faults that may serve as proxy examples for other areas. Finally, we derive a preliminary generic model for the origin of spectral gamma-ray variations in faulted sandstones, limestones, and metamorphic successions. This shows why fluid-rock interactions along bedding-parallel zones of deformation generate elevated K and U and depressed Th/K and Th/U. Our observations may aid subsurface studies of the complex stratigraphy below thrusts.

GAMMA-RAY AND SPECTRAL GAMMA-RAY LOGS IN STRATIGRAPHIC ANALYSIS

Gamma-ray or natural gamma-ray logs show stratigraphic variation in all gamma-ray radiation, regardless of isotopic source. Outcrop (Slatt et al., 1992) and borehole (Van Wagoner et al., 1990) spectral gamma-ray logs differentiate potassium (K), uranium (U), and thorium (Th), which may be used as proxies for certain mineral contents such as K-feldspar. Stratigraphic or depth variations in total gamma-ray, K, U, and Th are displayed on one log, commonly

Copyright ©2004. The American Association of Petroleum Geologists. All rights reserved.

Manuscript received September 5, 2003; provisional acceptance January 22, 2004; revised manuscript received March 10, 2004; final acceptance April 16, 2004.

AUTHORS

A. RUFFELL ~ *School of Geography, Queen's University, Belfast, Northern Ireland; a.ruffell@qub.ac.uk*

Alastair Ruffell has a Ph.D. (geology) from the University of Birmingham (United Kingdom). Prior to this, he was a geophysicist in Rio Tinto Zinc and Elf Aquitaine. An Imperial College (London) postdoctoral research led to a teaching position at Queen's University in Belfast. He is currently working on various aspects of clay mineralogy, including quantitative x-ray diffraction, uses of clay mineralogy in paleoclimate studies, the geophysics of clays (gamma-ray and ground-penetrating radar responses), and forensic geoscience.

J. M. MCKINLEY ~ *School of Geography, Queen's University, Belfast, Northern Ireland; j.mckinley@qub.ac.uk*

Jennifer McKinley has a Ph.D. (geology) from Queen's University (Belfast) on the petrography and geochemistry of reservoir variation. She is currently working on a postdoctoral research on spatial modeling of permeability in visibly homogenous sandstones. Research interests include use of geostatistics in the spatial analysis of mineral cements and fluid-flow properties of rocks.

R. EVANS ~ *Department of Petroleum Engineering at Curtin University, Curtin, Perth, Western Australia; richarde@peteng.curtin.edu.au*

Richard Evans is a research fellow in reservoir characterization at Curtin University of Technology, where he also lectures on formation evaluation and 3-D reservoir modeling. He was awarded a Ph.D. from the Queen's University of Belfast (1998) for research on Carboniferous outcrop analogs in the north of Ireland region. This was followed by two Shell/Exxon-sponsored postdoctoral projects at Imperial College of London and Cardiff University on the seismic architecture, evolution, and faulting of the Tay Fan, United Kingdom, in the North Sea. Before joining Curtin in early 2003, he worked as a consultant geoscientist for Reservoir Management Limited in Aberdeen, working on a variety of industry projects in the North Sea and west of Shetland basins. He is interested in the multidisciplinary characterization of reservoir and aquifer rocks from

pore throat to basin scale, to investigate the controls on reservoir architecture, porosity, permeability, and fluid flow for static and dynamic modeling. He is currently working closely with Commonwealth Scientific and Industrial Research Organization and Woodside Energy Limited on several joint research projects.

ACKNOWLEDGEMENTS

We thank Lindsay Proudfoot, Brian Whalley, and Luis Pomar for their help at Estellences in Majorca. We thank Evgenij Baraboshkin and Andre Guzikov for organizing the Ukraine trip. We also thank Richard Worden, Chris Cornelius, and John Meneely for help with fieldwork at Mullaghmore and laboratory analyses. The Neoproterozoic study was carried out by Matt Hadley and instigated by Graham Leslie and Bernard Anderson, the latter provided other fault details, for which he is thanked. Many thanks to Pedro Rios and Dale Leckie for providing information on the Guando field. This paper was improved by the helpful reviews of Laura Foulk, Roger Slatt, and Laird Thompson.

with ratios of Th/K and Th/U. Peaks, troughs, and the overall shape (or motif) of these logs have been used as a method of identifying the surfaces and bedding cycles (e.g., parasequences) on which sequence-stratigraphic analyses are based (Van Wagoner et al., 1990; Davies and Elliot, 1996). A recent (2003) search of published literature on gamma-ray logs in stratigraphic analysis demonstrates how routine and widely used this logging technique has become (e.g., George, 2000; Svendsen and Hartley, 2001). In addition to these interpretations of basin-fill architecture, facies prediction, and hydrocarbon exploration, spectral gamma-ray logs have also been used to aid in structural correlation (Hadley et al., 2000), strata-bound orezone definition (Juodvalkis and Barnett, 1997; Ruffell et al., 1998), paleontology (Hardenbol et al., 1998), and diagenesis (Ketzer et al., 2002). Most importantly for this work, spectral gamma-ray logs are widely used for correlation and petrophysics in downhole and outcrop studies, sometimes with only limited acquisition of core or in areas of limited outcrop, where bedding-parallel tectonic dislocations, such as thrusts, slides, and deep listric faults, may be common but not easily observed.

SPECTRAL GAMMA-RAY EMISSION

The usefulness of spectral gamma-ray data originates with mineralogical variation controlling the sites in which K, U, and Th may reside. K is common in many sediments that bear K-feldspar, muscovite micas (and others), clays, or salts. K is known to be leached from feldspars and muscovite during kaolinite formation. Th is only partly soluble and may be concentrated relative to K and U during their removal (Parkinson, 1996). U and Th have several host minerals in sedimentary rocks, including clays, feldspars, heavy minerals, phosphates, and organic matter. Specific heavy minerals have high Th or U contents (Hurst, 1990), creating a potential problem in interpreting the gamma-ray emission of sedimentary rocks containing zircons, detrital uraninites (UO_2) or thorites ($ThSiO_4$). U is soluble and thus more prone to mobilization than Th during leaching and clay mineral diagenesis. Th/U ratios from shallow-buried mudstone-rich successions may show similarities to Th/K ratios, if the U is also being preferentially leached during hinterland weathering or postdepositional diagenesis (Osmond and Ivanovich, 1992; Rosholt, 1992). Gamma-ray logs cannot automatically be used as a simple proxy for grain size because of the complications caused by the presence of heavy minerals (Hurst, 1990), K-rich feldspars, anoxia (Myers and Wignall, 1987), and carbonate contents (McRoberts et al., 1998).

FAULTS AND GAMMA-RAY EMISSION

Faults and fault zones may be associated with mineralizing fluids and the formation of argillized rock flour or fault gouge. Fluids,

moving through fault zones and precipitating minerals may be of higher temperature and chemistry to the country rock and thus have the capability to mobilize and concentrate K, U, and Th. Both K-feldspars and uranium oxides in faults and fracture zones have been routinely detected using spectral gamma-ray surveys (Sikka, 1962). Th is mobilized and concentrated in the presence of humic acids from organic matter. The resulting Th-enriched bitumens may be detected on spectral gamma-ray logs (Dutkiewicz, 2001). The formation of fault gouge increases the surface area of minerals that may either adsorb large atoms such as U and Th or alter their mineralogical state and increase K, U, or Th incorporation. The presence of K-, U-, or Th-enriched, hydrothermally mineralized or fine-grained rock in faults is therefore highly likely. The reason why the association between fine-grained, possibly radioactive material in bedding-parallel (to subparallel) faults is of interest to the reservoir geologist is examined below. The concentration of K, U, and Th in the finer grained fraction of rocks is one of the main premises behind the original use of gamma-ray logs in stratigraphic analysis. In clastic-dominated successions, fine-grained deposits are commonly deposited during periods of decreased depositional energy, especially during transgressions. K is found in fine-grained K-feldspar and illite. U is found adsorbed onto clay minerals and associated with organic matter, which is also concentrated in finer grained rocks. Th is common in illites and biotites, again in the fine fraction of rocks. Fine-grained fault gouge in reservoir conglomerates, sandstones, and limestones may show elevated K, U, or Th that is unrelated to stratigraphy. This is not a problem if the fault is identified in core, from formation scans, or through correlation to seismic data. The types of faults that are likely to remain undetected are subparallel to bedding in poorly dated successions, where there is no evidence of repeated or missing stratigraphy. Bedding-parallel faulting is common along suitable mechanical surfaces such as shales in sandstones that have been subject to tectonism. Thus, many fine-grained beds in a succession may have had slip along them that has altered mineralogy and thus K, U, and Th contents. Here, we document the spectral gamma-ray response across rocks with proven deformation; further work may differentiate between stratigraphic bounding surfaces that have slipped and those with no movement. During spectral gamma-ray logging, we have encountered faults, many of which had a dramatic effect on the spectral gamma-ray data (see below). This study shows four tectonic dislocations that are subparallel to bedding (Figure 1a–e) and thus potential proxies for the type of cryptic surface that others may encounter at outcrop or downhole and possibly confuse with important stratigraphic surfaces (as we did in our initial studies). We also document a high-angle normal fault (Figure 1f–h) that does not show such dramatic and potentially misleading spectral gamma-ray variation. All the case studies have been chosen to document a range of sedimentary and low-grade metamorphic successions that are relevant to the reservoir geologist. Limited cliff outcrops may be similar in dimension to borehole core, resulting in misidentification of a potential flooding surface. Our work characterizes the spectral gamma-ray emission of both bedding-parallel and bedding-oblique faults, with cautionary examples from thrusts that will serve as possible interpretation proxies for other studies.

METHODS

Over the 5 yr taken to complete this study, 80% of the measurements were made using a Scintrex GIS-5 machine, calibrated to a Th standard and deployed at a 30–50 (12–20-in.)-cm sample distance. The methodology of Slatt et al. (1992) was followed, wherein five readings were taken at each site, the lowest and highest were discarded, and the three remaining were averaged. Machine availability and cross-validation allowed additional measurements to be taken using an Exploranium GR256 Spectrometer. This device automatically calculates K, U, and Th contents and Th/K and Th/U during the 4-min recording time at each location (Davies and Elliot, 1996). Clay mineralogical analysis was conducted by x-ray diffraction, using a Siemens D-5000 diffractometer on crushed whole rock samples for quantitative analysis using the method of Sródon et al. (2001). Mineralogical analyses are quoted where appropriate because they are not the main focus of this work but do sometimes indicate the origin of a particular gamma-ray measurement. In each case study, we describe the sedimentological and structural origin, spectral gamma-ray logging results, and end with a short interpretation.

CASE STUDIES

Sandstone Case Study I: Triassic Bunter Sandstones, Northern Majorca (Western Mediterranean)

The northern mountains of the Spanish Mediterranean island of Majorca (Sierra Norte or Serra de Sierra Tramuntana) expose a fold and thrust belt of

Mesozoic–Paleogene rocks that have sedimentological and structural affinities to the Betic Cordillera of southeastern Spain (Gelabert et al., 1992). In the Sierra Norte, a stratigraphically complete Triassic succession (Alvaro, 1987) of Bunter, Muschelkalk, and Keuper (with Jurassic limestones above) can be observed in the cliffs between the fishing port and village of Estellences (lat. 2°30′20″, long. 39°40′10″). A review of the depositional conditions of the Bunter Sandstone in Majorca, based largely on this location, can be found in Gómez-Graz and Alonso-Zarza (2003). The thrusted succession examined here comprises more than 50 m (160 ft) (vertical succession) of interbedded medium-grade dark red to chocolate brown sandstones, nodular carbonate-cemented sandstones, and intraformational conglomerates (clasts comprise mixtures of reworked

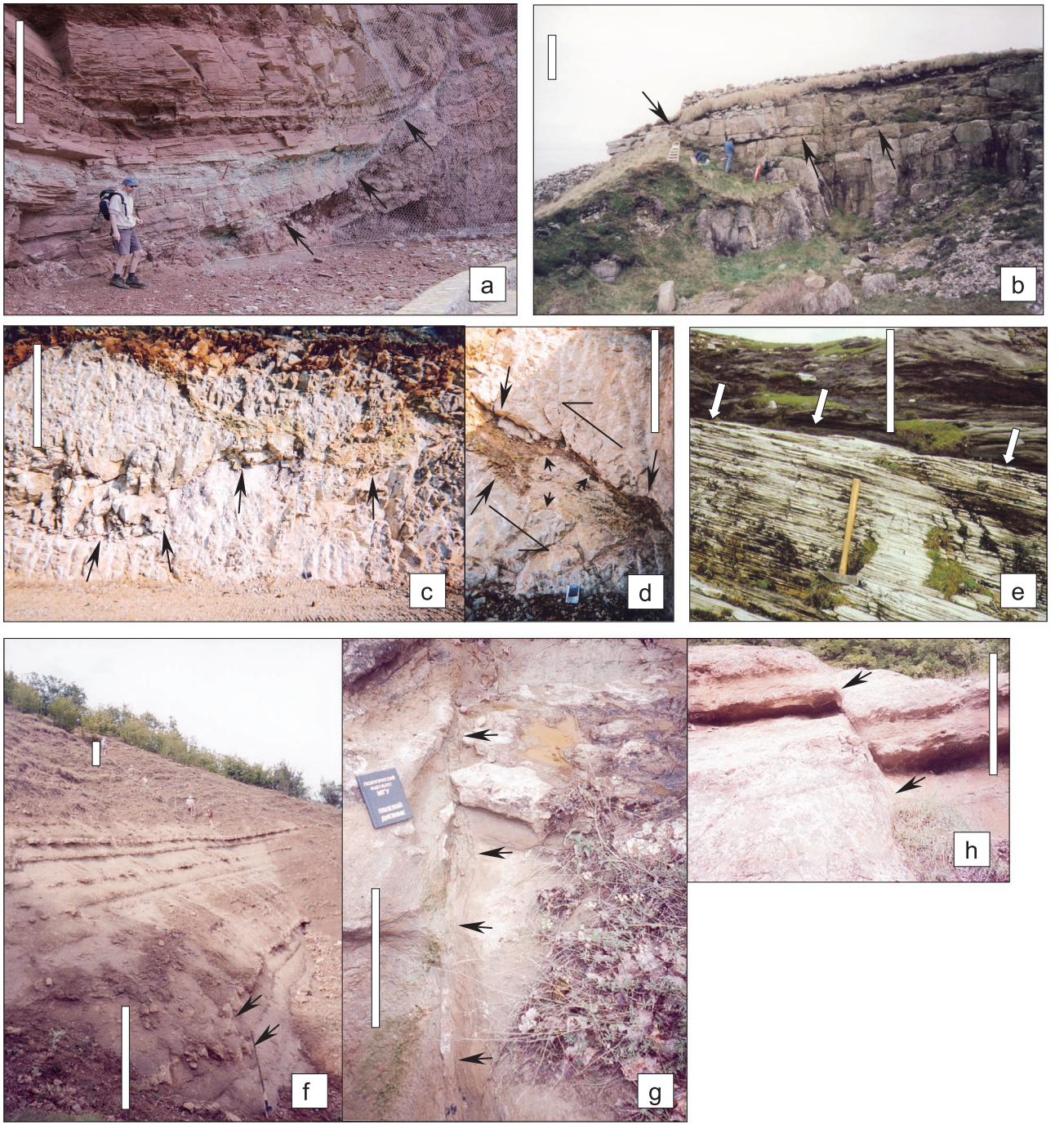

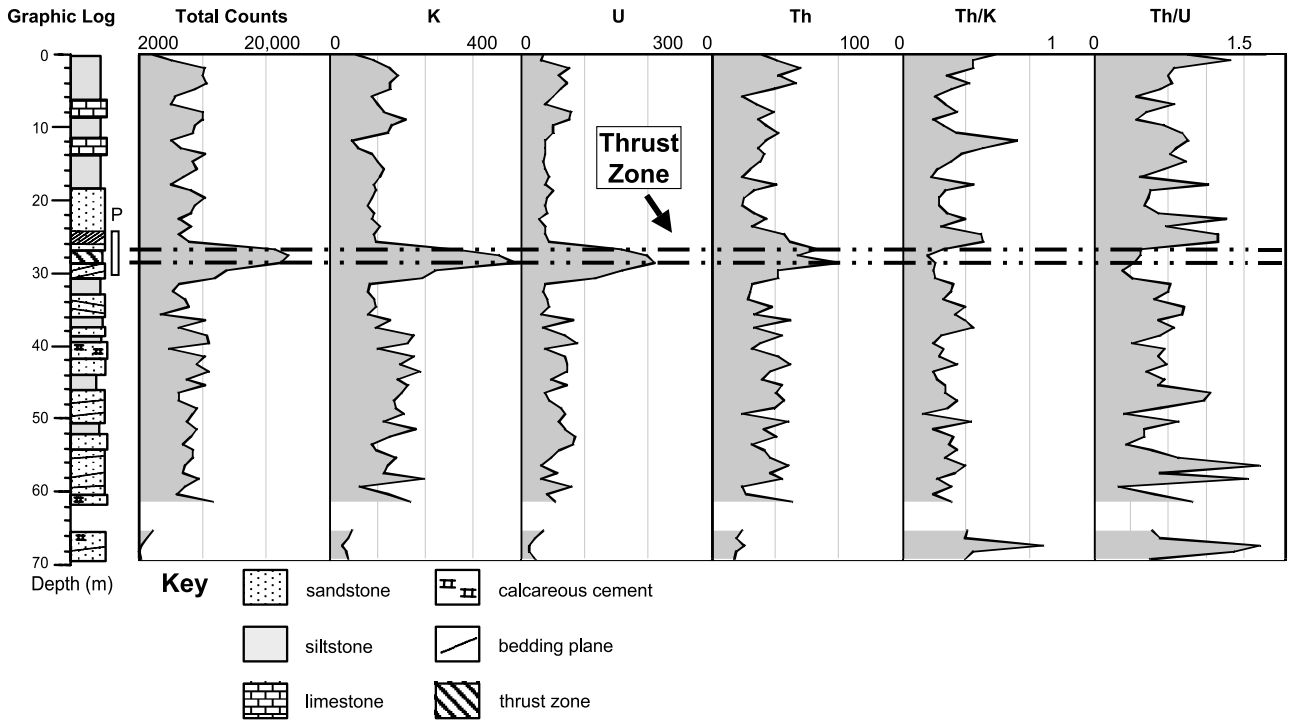

Figure 2. Spectral gamma-ray log of the Lower Triassic (Bunter Sandstone dot ornament) and Middle Triassic (Muschelkalk silt, clay, and limestone ornament) at Estellences, northern Majorca. The stratigraphic location of section photograph in Figure 1a is indicated by P on the lithologic log. The upper and lower limits of the thrust zone arrowed correspond to all the deformed beds above and below the thrust, not just the high radioactivity green bed itself.

mud flakes and carbonate nodules; Gómez-Graz and Alonso-Zarza, 2003). A 30–90-cm (12–35-in.)-thick gray-green, weathered-back bed cuts through the middle part of the Bunter Sandstone stratigraphy (arrowed in Figure 1a). During gamma-ray logging, anomalously high emissions of all natural radioactivity were noted from the 30- to 90-cm (12- to 35-in.)-thick gray-green bed (Figures 1a, 2) and from 5- to 10-cm (2- to 4-in.)-thick green beds as much as 2 m (6.6 ft) below. Th/K and Th/U ratios demonstrate that K and U abundances are more than double that of enclosing red sandstones (Figure 2). The fault gouge that displays high radioactivity is a slaty clay with fibrous texture. X-ray diffraction and thin-section analysis demonstrate that the

Figure 1. Photographs of the faulted and other tectonically disturbed successions described in text. (a) View from northeast to southwest of the thrusted Bunter Sandstone (Triassic) succession at Estellences (northern Majorca, Balearic Islands, western Mediterranean). Scale bar is 2 m (6.6 ft). Arrows mark the line of the main high-radioactivity thrust zone, here filled with a fibrous green illite clay. Elevated gamma-ray emissions also occur in green horizons with a slaty fabric above and below. (b) Photograph from south to north of the quarry on Mullaghmore Head (County Sligo, Ireland) in Carboniferous Mullaghmore Formation sandstones. Scale bar is 2 m (6.6 ft). Arrows mark the stylotized, high-radioactivity bed. (c) Photo taken facing north of the dip view of south-dipping thrust (arrowed) in Jurassic limestones, Santa Ponsa, southwest Majorca. Scale bar is 2 m (6.6 ft). (d) Strike view of the same thrust (c) in Jurassic limestones, Santa Ponsa (Majorca). In adjacent (smooth) weathered cliffs, this thrust forms a vegetated and weathered-back indentation that is indistinguishable from bedding planes. Half-arrows show the sense of movement indicated by folds in the limestone block (small arrows mark the edge) in the thrust zone. (e) Detail of the Horn Head Slide (arrowed) at Micky's Hole, Horn Head, County Donegal (Ireland). View faces south; hammer and scale bar are 35 cm (14 in.) long. Courtesy P. McKeevar, Geological Survey of Northern Ireland. The lineation visible in the quartzite below the slide is formed by stretched pebbles, coincident with elevated gamma-ray emission. (f–h) Views of Hauterivian (Lower Cretaceous) sandstones exposed in a stream tributary of the Kacha River Valley (southwest Crimea, Ukraine). (f) Overview of the bedded Hauterivian sandstones with part of the most faulted section at the base of the photograph (adjacent to long shovel). Scale bars (foreground and on hill) are both 2 m (6.6 ft). (g) Detail of fault gouge. Scale bar is 50 cm (20 in.). (h) Detail of normal fault with no visible fault gouge. Scale bar is 1 m (3.3 ft).

fault gouge is dominated by muscovite with minor (less than 5%) talc. Thin green beds below the thrust also show a slaty fabric and are composed of muscovite. Prior to petrographic analysis, we interpreted the green, cross-cutting bed as the base of a channel because when logging (1999 and 2000) at close proximity to the rocks, the overall geometry was not clear. Had this succession been only observed in a borehole core, the thrust would not be obvious. With removal of rubble in 2002, during construction of a cliff path, a long view was possible, and the geometry of the thrust became clear. Thus, our stratigraphic interpretation became a tectonic one, demonstrating how easy it is to confuse the two possible origins of elevated K and U emission in limited outcrop or core.

Sandstone Case Study II: Carboniferous Mullaghmore Sandstone, Quarry Section, County Sligo (Northwest Ireland)

This study concentrates on a sandstone succession exposed in a 20-m (66-ft)-long-by-3-m (10-ft)-high face in a disused quarry (Figure 1b) on the northwest coast of Mullaghmore Head, County Sligo, Ireland (lat. 8°29′10″, long. 54°28′0″). The rocks exposed in this quarry form part of the Lower Carboniferous Mullaghmore Formation (Ketzer et al, 2002), which in North Sligo is estimated to be 197 m (646 ft) thick and comprises rhythmically bedded mudstones, siltstones, and sandstones deposited in the northwest Carboniferous basin (Ireland; Price and Max, 1988). This basin has a tectonic history of synsedimentary extensional tectonics, followed by deep burial and heating that was synchronous with Variscan (end Carboniferous) compressional deformation. Northeast-southwest–oriented thrusts with hundreds of meters of lateral displacement are documented as close as 15 km (9 mi) from the study site (Mitchell and Owens, 1994). Millar (1990) documents decimeter-thick, weathered-back, soft silty sandstone beds that were intensively fractured and stylotized during Variscan compression. The succession studied comprises gray, medium-grained sandstones with low-angle cross-stratification, low-relief erosional channels, and silty sand layers. A visually striking weathered-back (arrowed in Figure 1b) and intensively stylotized (stylolites are 2–5 cm [0.8–2 in.] apart) siltstone-sandstone layer (10–15 cm [4–6 in.] thick) occurs in the studied section. The stylolites are orientated parallel to sedimentary bedding and are also abundant in adjacent silty sandstone beds where interconnecting anastomosing networks of stylolites were observed. Mica and illite-rich stylolite veins range from 0.10 to 0.4 mm (0.004 to 0.02 in.) and cause sutured contacts with surrounding quartz and feldspar clasts. Opaque minerals are seen to be concentrated in the stylolites. Sandstone-siltstone-mudstone bedding cycles above and below the stylolite-rich bed are reflected in rhythmic peaks and troughs on the total-count gamma-ray logs (Figure 3). These appear to be the result of fluctuating U and Th. The presence of heavy-mineral layers in lag deposits has been noted (Ketzer et al., 2002) and may help explain this distribution. K emissions show a gradual increase toward the stylolite-rich bed, with a dramatic fall above (Figure 3).

The cyclic nature of the Mullaghmore succession lends itself to a sequence-stratigraphic interpretation of retrogradational and then progradational parasequences (Figure 3), with a gamma-ray peak that would conventionally be interpreted as a flooding surface (Figure 3) generated by K and U peaks. This is apparently confirmed by the low Th/K and Th/U ratios, when compared to Davies and Elliot (1996). Elevated spectral gamma-ray measurements (high total, K and U counts, and low Th) are coincident with the weathered-back stylotized bed, demonstrating how easy it is to confuse this deformed bed with a flooding surface. Gamma-ray emission and stylotization in the enclosing sandstones both increase above and below the weathered-back bed.

Limestone Case Study: Jurassic Platform Carbonates, Southwestern Majorca (Western Mediterranean)

The limestone succession exposed in the far west of Majorca is part of the Sierra Norte fold and thrust belt mentioned in sandstone case study I (Gelabert et al., 1992). The limestones examined here comprise the post-Pliensbachian (early Jurassic) pelagic facies of Jenkyns et al. (1990). The succession studied is in the cliffs on the northern side of Santa Ponsa Bay (Cala de Santa Ponsa, lat. 2°30′10″, long. 39°32′0″). Here, an asymmetric anticline, with a northeast-southwest–oriented axis, brings Jurassic strata to surface in a tectonic window of Cretaceous limestones (Ministerio de Industria, 1972). This anticline lies in the footwall to the easternmost mapped thrust of the Sierra Norte. A smaller, southeast-dipping thrust is exposed in a series of quarries and building excavations in the cliffs north of Santa Ponsa Bay (Figure 1c, d). Limestones here comprise decimeter-thick beds of oolitic, stromatolitic, and pelletal dolomitized rocks, interpreted to be part of an oceanic carbonate platform (Jenkyns et al., 1990). Both the thrust and bedding planes dip 30–40° to the

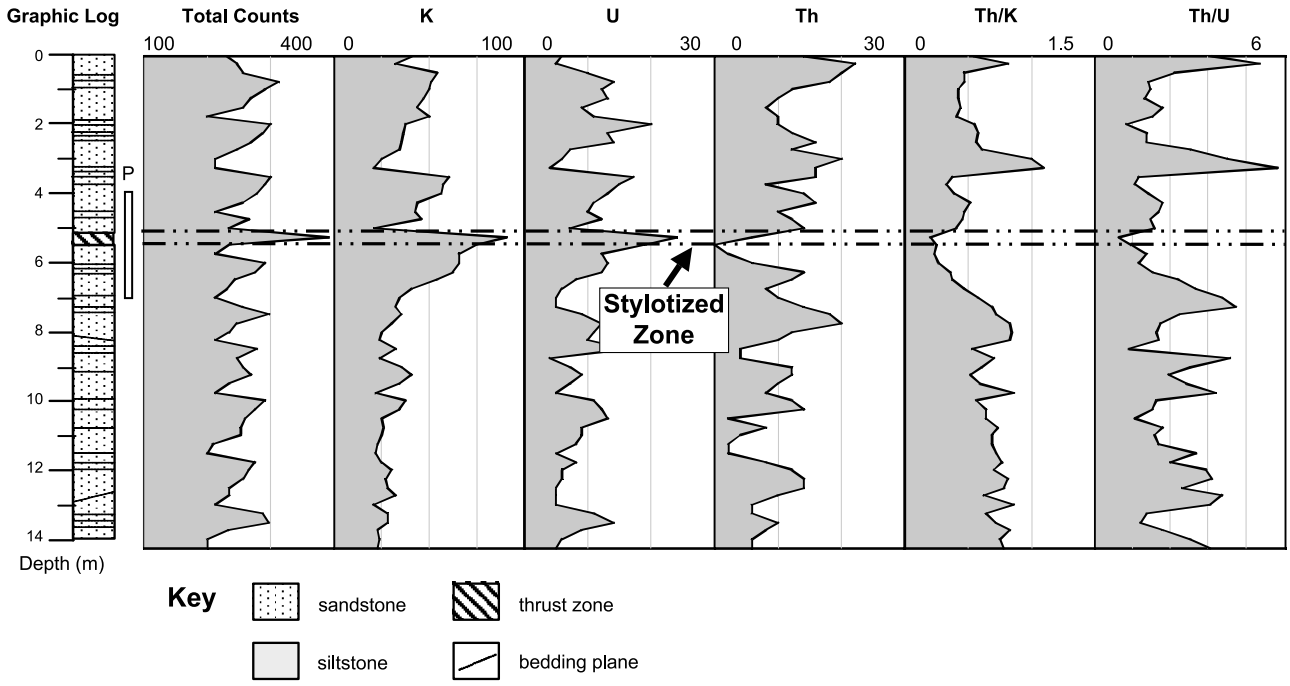

Figure 3. Spectral gamma-ray log in the upper third of the exposed Mullaghmore Sandstone Formation (Carboniferous) at Mullaghmore Head (County Sligo, Republic of Ireland). The stratigraphic location of section photograph in Figure 1b is indicated by P on the lithologic log. The stylotized zone extends 10–30 cm (4–12 in.) into the sandstones below the weathered-back bed.

south and are characterized on weathered cliffs by lines of vegetation, rendering the two visually indistinguishable. Fortuitously, foundation excavations made during holiday apartment construction have created regular fresh exposures, where thrusts and bedding can be mapped (Figure 1c, d). The thrust zone in the excavation measured displays undulating upper and lower contacts with the limestone, dips at 30° to the southeast, and is 60–80 cm (24–31 in.) thick. The zone is filled with a mixture of 3–4-cm (1.2–1.5-in.)-long angular limestone (breccia) clasts, floating in a fine-grained matrix. X-ray diffraction analysis of the silt- and clay-grade fraction of this cataclastite demonstrated the presence of (approximate quantities) dolomite (52%), smectite (28%), calcite (14%), and quartz (5%). The elongate breccia clasts provide a thrust-parallel fabric to the zone. A strike view of the thrust shows that the overthrust limestones are massive, with decreasing numbers of centimeter- to decimeter-spaced fractures. The limestones below the thrust are chalky and also show fracturing close to the thrust that is not apparent in the cliff below. Over 100 m (330 ft) of limestones are exposed in the Santa Ponsa section, of which 60 m (200 ft) were logged. Above and below the thrust zone, all the spectral gamma-ray information display cyclicity best seen on the K log (Figure 4). The thrust zone displays a significant total gamma-ray peak that the spectral data show to be caused by U and Th contents. Low Th/U shows U to be the dominant contributor to the total count in the thrust zone. K is elevated 6 m (20 ft) above and below the thrust zone (Figure 4).

Ehrenberg and Svånå (2000) summarize the few works that document the spectral gamma-ray response of carbonates. Their summary indicates that K and Th reflect clastic content, with U concentration determined by late diagenetic processes (for example, see the work of Lucia, 1999). This is vindicated by the present study. One surprise, however, from both Ehrenberg and Svånå's (2000) summary and this work is the comparison to McRoberts et al. (1998), who showed that Th contents in limestones may be influenced by carbonate dilution. In our case, the fall in spectral gamma-ray Th content in (and for 1 m [3.3 ft] above) the clay-rich thrust zone (Figure 4) is the opposite of the expected results from McRoberts et al. (1998) and yet the same as those from Ehrenberg and Svånå (2000). Logging of this section in core, or without the benefit of the quarries and excavations on weathered cliffs, could easily miss or misinterpret the thrust, it being parallel to bedding. Thus, the gamma-ray peak and Th/U (and also Th/K) could be interpreted as a flooding surface, the high U content of which may indicate (wrongly) the presence of

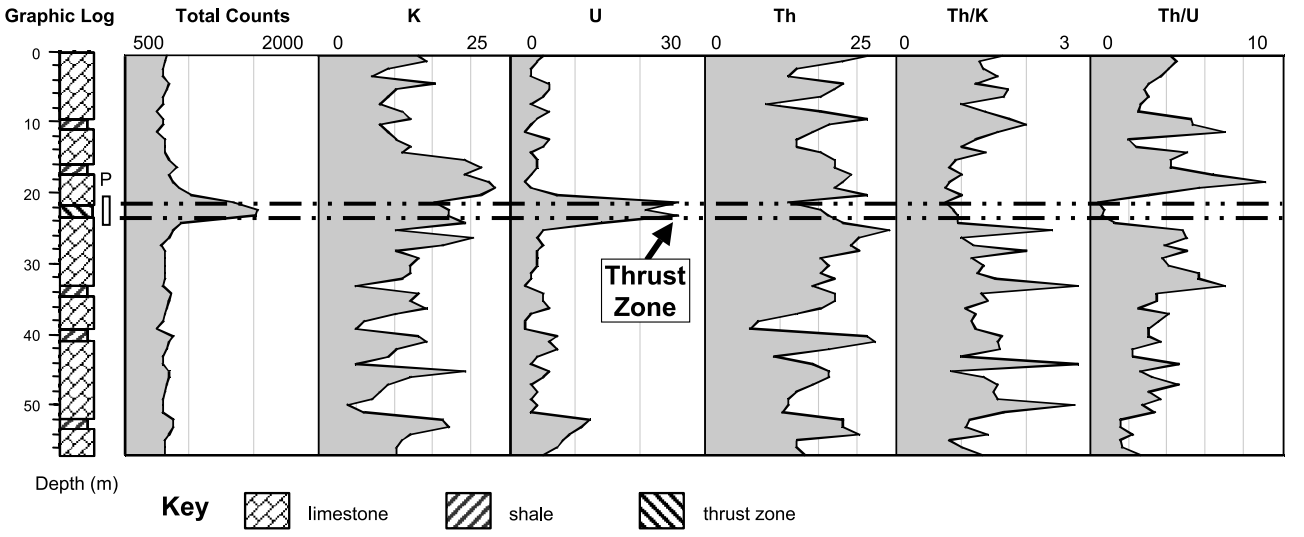

Figure 4. Spectral gamma-ray log through the Jurassic platform limestones exposed in the cliffs north of Santa Ponsa Bay (Majorca). The stratigraphic location of section photograph in Figure 1e is indicated by P on the lithologic log.

organic matter (Myers and Wignall, 1987). Instead, we propose that the Neogene movement of the thrust (Gelabert et al., 1992) caused contemporaneous brecciation, dissolution of carbonate, and concentration of organic matter and clay onto which U was adsorbed following carbonate removal.

Metamorphic Case Study: Neoproterozoic Appin Group Quartzites and Pelites, Donegal (Northwest Ireland)

When gamma-ray logs were first interpreted in terms of depositional sequences (Van Wagoner et al., 1990), shallow-buried, mildly deformed, and unmetamorphosed successions were studied. The passage of hydrothermal fluids through rocks during metamorphism would intuitively imply mobilization of K, U, and possibly Th, such that the original depositional gamma-ray signal would be lost. However, the work of Juodvalkis and Barnett (1997) was pioneering in demonstrating that although significant gamma-ray variation could be expected in metamorphosed successions, commonly, the redistribution of K, U, or Th mirrored what was to be expected from unmetamorphosed sequences. Thus, Hadley et al. (2000) demonstrate (from the succession described here) the low gamma-ray counts from quartzites (originally sandstones) and elevated K and U emissions from pelites (originally mudstones) that would be expected in unmetamorphosed successions.

The Neoproterozoic Dalradian Supergroup succession exposed in County Donegal (northwest Ireland) comprises a series of marine metasediments deposited, deformed, and intruded by dolerites and granites contemporaneously with rocks of the Scottish Highlands and Pennsylvanian fold belt (Long and McConnell, 1997). The main tectonic phase affecting the Donegal succession is that of the Caledonian orogeny, when polyphase deformation caused low-angle dislocations or slides to cut the succession, both excising and repeating stratigraphy. These slides were later folded and faulted themselves. The tectonics and gamma-ray spectroscopy of the slide used in this study have been documented before (Hadley et al., 2000); the stratigraphic formation above the slide is the subject of discussion (Long and McConnell, 1997). The present study concentrates on the stratigraphic distribution of spectral gamma-ray variation across the slide horizon, exposed at Micky's Hole on the Horn Head Peninsula (lat. 8°10′0″, long. 55°15′10″). Here, quartzites of the Ards Quartzite Formation are overlain by pelites of unknown affinities; adjacent to the Horn Head Slide, pebbles in the quartzites become highly stretched, and the pelites display a pervasive slide-parallel fibrous fabric (Figure 1e). The pelites and quartzites contain micas that can host K, whereas the pelites are dark in color, suggesting an iron or organic matter content that may host U. Quartzites below the slide show no exceptional spectral gamma-ray variations, with total counts remaining just above 600 (30-s count times), K and U showing some rhythmic fluctuations, and Th displaying one prominent double-headed peak that produces a spike in the Th/K and Th/U ratios (Figure 5). From 3.5 m (11 ft) below to the Horn Head Slide itself, total-count gamma-ray radiation and K rise in tandem with an increasingly prominent stretching fabric in the quartzites.

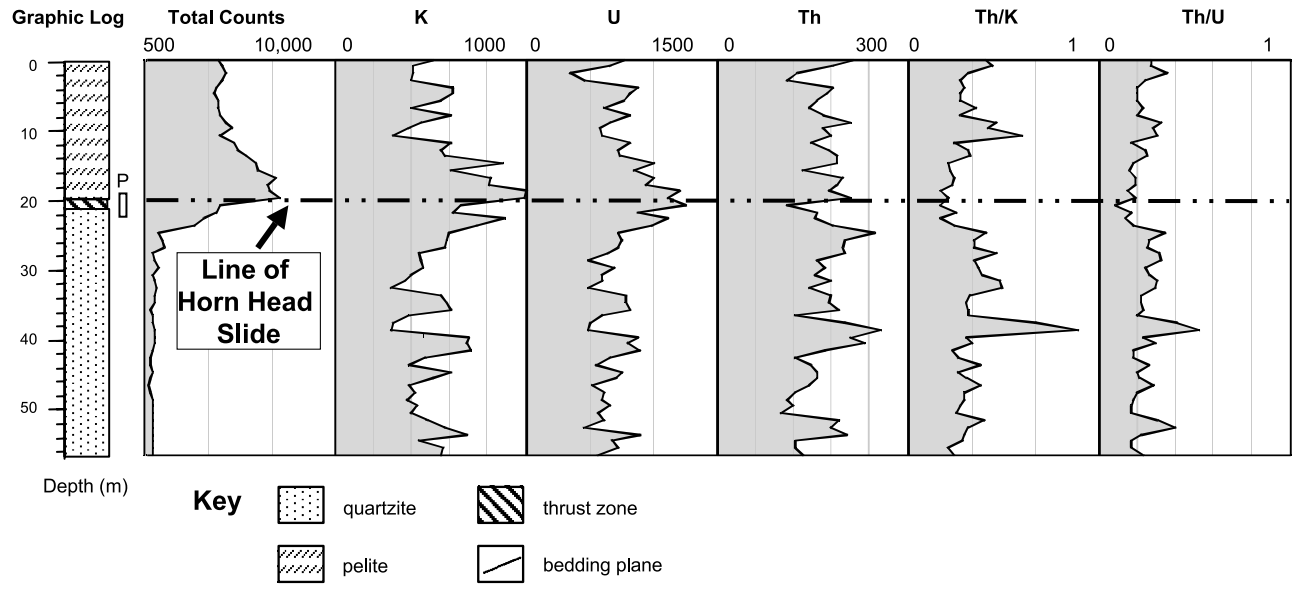

Figure 5. Spectral gamma-ray log through the Ards quartzites (stipple), slide zone, and overlying pelites exposed at Horn Head (County Donegal). The stratigraphic location of section photograph in Figure 1a is indicated by P on the lithologic log.

Hadley et al. (2000) demonstrated that K is the dominant radioactive isotope in the overlying pelites, suggesting downward redistribution from the slide. From 4 m (13 ft) below to 1 m (3.3 ft) above the slide, Th emissions fall by about 60%, rising again in the pelites some 1–2 m (3.3–6.6 ft) above the slide (Figure 5).

The application of the principles of spectral gamma-ray stratigraphy shows that a jump in average total-count gamma-ray values from quartzites to pelites would be expected, such as one may encounter at a flooding surface or where quartz sand clastic supply was diminished in the original sedimentary environment. However, we note that the quartzites 3 m (10 ft) below and pelites 7–8 m (23–26 ft) above the Horn Head Slide show elevated gamma-ray emissions (Figure 5). The nucleation of the slide at a previously hot horizon in the pelites is likely given that such horizons may commonly coincide with surfaces of structural weakness or ductile materials. The elevated gamma-ray signal in the quartzites below the slide is anomalous. Perhaps fluid flow and mineralization associated with the slide may have concentrated K and U preferentially in the overlying pelites and underlying quartzites.

Sandstone Case Study III: Cretaceous (Hauterivian) Sandstones Belaya Mountain, Kacha River, Southwest Crimea (Republic of the Ukraine, Northern Black Sea)

The postmetamorphic (basement) geology of southwest Crimea comprises a succession of rift, postrift, and compressional foreland basin sediments that were deposited in the western Black Sea Basin succession (Nikishin et al., 1998). Throughout the Mesozoic, tectonic activity was controlled by the differential movement of the Arabian platform to the south, Scythian platform to the northeast and East European platform to the north. The Cretaceous succession examined here lies in the Great Caucasus–southern Crimea orogen (Nikishin et al., 1998), much of which is folded and thrusted. However, the Lower Cretaceous sandstones examined dip at 5–10° to the west and north throughout the area. The succession is described by Baraboshkin (1999) and Khryashchevskaya and Baraboshkin (2001). Some descriptions are given in Gröcke et al. (2003). However, there are few published accounts of the whole stratigraphy.

The studied fault zone intersects north-dipping Hauterivian sandstones exposed in a small river on Belaya Mountain in the Kacha River Valley, Verkhorechie village (lat. 33°45′00″, long. 44°50′10″). The fault zone strikes approximately east-west and is thus strike parallel. Faults are predominantly normal, downthrowing to the south. Most contain a thin fault gouge, resulting in small gorges, commonly filled with debris and vegetation (Figure 1f–h). However, in the river valley itself, the high rate of erosion keeps the fault zone and individual fault fills swept of debris, allowing clear examination. The entire succession was measured, including a vertical fault zone that influences about 8 m (26 ft) of strata. Some faults show no gouge and

clear bed-to-bed contacts (Figure 1h). One, in particular (Figure 1g), has a 15–40-cm (6–16-in.)-wide gouge filled with fine-grained material. Subsequent x-ray diffraction analysis of this gouge demonstrated the presence of smectite, biotite, quartz, illite, chlorite, mixed-layer clays, and glauconite. This is essentially the same mineralogy (with less quartz) as the surrounding rock. Gamma-ray logs of the succession were made using a measurement spacing of 30 cm (12 in.), in tandem with magnetic susceptibility measurements made by a team from Saratov University for stratigraphic correlation. The total-count data demonstrate the clear influence the faulted strata have on the gamma-ray log (Figure 6). This broad peak is the result of combined K- and Th (minor U)-sourced radiation. To examine whether this is true for individual faults, the clearest fault with gouge (Figure 1g) was measured in detail, where elevated total counts, K, and Th were confirmed. These data contrast with that from thrusts and strike-slip faults (Table 1), which show a fall in Th/K and Th/U; the Crimean normal faults instead show peaks in Th/U and Th/K (Figure 6). Van Buchem et al. (1992) suggest that simultaneous stratigraphic changes in K and Th are most likely caused by fluctuations in illite content. We have observed comparable variations in K and Th across faults where there is a dominance of illite in the gouge. The important point for this study is that the Crimean sandstone example is dissimilar to the previous examples in that the fault zone, although possibly mirroring a flooding surface or condensed section from total-count data alone would not be confused for such when the Th/K and Th/U ratios are examined.

DISCUSSION: DEVELOPMENT OF MODEL

The intentionally diverse range of thrusts, low-angle faults, deformed beds, and slide described in this work show similarities implying that a preliminary genetic model may be developed. These similarities include elevated total count, K and U gamma-ray radiation; moderate Th enrichment; or, more commonly, depletion

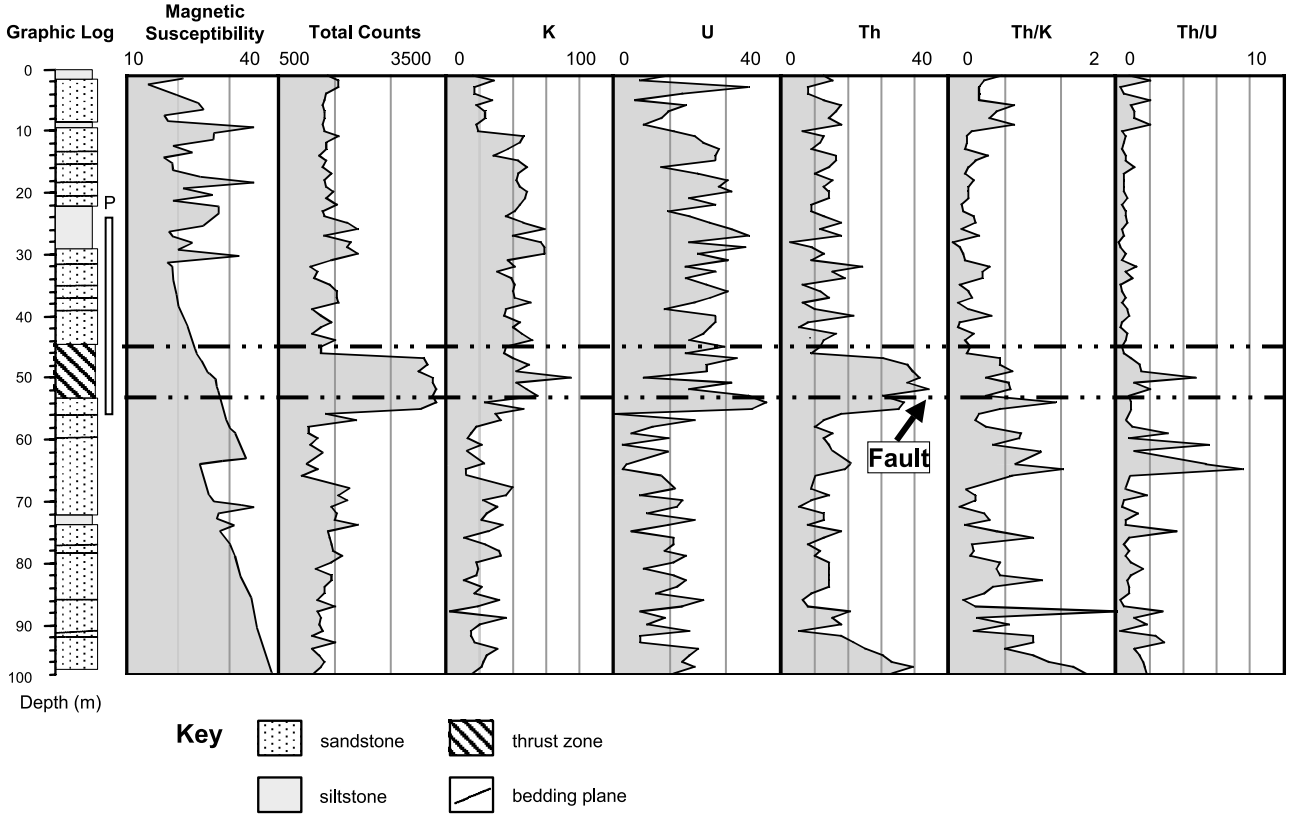

Figure 6. Spectral gamma-ray log through the Hauterivian (Lower Cretaceous) sandstones exposed in the Kacha River Valley (southwest Crimea), including the faulted zone. Note how this fault zone shows no effect on magnetic susceptibility (data courtesy of A. Guzhikov, Saratov University). The stratigraphic location of section photograph in Figure 1f is indicated by P on the lithologic log.

Table 1. Strike-Slip Faults Measured Using a Spectral Gamma-Ray Device as Background to this Study

Location	Description	TC	K	U	Th	Th/K	Th/U
1 km (0.6 mi) east of Watchet, United Kingdom lat. 3°18′45″, long. 51°10′40″	anastomosing network of calcite veins some 3 m (10 ft) wide on a strand of the Watchet Cothelstone fault; displacement here probably Tertiary dextral, displaces Jurassic shales and limestones	10% lower than surrounding shales	5% (negligible) lower than country rock shales	10% lower than shales	negligible	0.9	0.8
Triscombe, Somerset, United Kingdom lat. 3°11′40″, long. 51°6′40″	1-m (3.3-ft)-wide clay gouge in illite-chlorite grade metamorphosed deltaic Devonian sandstones; Variscan age movement	30% elevation	20% elevation	20% elevation	5–10% elevated	0.2	0.4
Orlock, County Down, northern Ireland lat. 5°34′10″, long. 54°40′00″	about 100-m (330-ft)-wide fault zone, mylonitization at the center, cuts Silurian graywackes; Caledonian age	20% elevation at margins of fault, 5% fall in center	TC elevation caused by 20% higher K	10% elevation at margins	10% elevated in center	average 0.8	average 0.9

and low Th/K and Th/U ratios. These are the same characteristics displayed by flooding surfaces on parasequences and at the maximum flooding surface itself. When the thrust or slide is well exposed, then this should not present a problem, but where subtle or poorly exposed, or downhole with no associated core, any type of low-angle or bedding-parallel tectonic dislocation or zone of fracturing could be mistaken as a flooding surface on spectral gamma-ray logs. Indeed, given the rheology of many rocks, it may be that many flooding surfaces have had their spectral gamma-ray output increased by being planes of weakness, decollement horizons, or areas of increased fluid movement and mineralization that concentrate K, U, and sometimes Th. We recommend caution in the interpretation of spectral gamma-ray logs from successions where bedding-parallel faults may be expected and the microscopic return to horizons of increased gamma-ray radiation to check for stretching lineations, fractures, and stylolites. Our model suggests that thrusts and other bedding-parallel zones of deformation show very similar, if not identical, spectral gamma-ray signatures to flooding surfaces.

This work is based on studies of outcrops with limited lateral exposure that are comparable to the amount of rock observed in core. Cursory examination of published work on spectral gamma-ray logs from boreholes in thrust-faulted successions shows that our work may equally be applied to the subsurface. Kimura et al. (1997) show the results of Ocean Drilling Program (ODP) Leg 170 (Costa Rican wedge), where faults intersect and duplicate Pleistocene–Pliocene silty clays and diatom ooze. The spectral gamma-ray data are similar to that recorded here in the limestone study; the ODP leg was lucky to have both good core recovery and detailed biostratigraphy that indicated the repetition of stratigraphy across the fault zone. Without either of these, information from spectral gamma-ray data alone could result in the fault being justifiably confused for a flooding surface. Coincidentally, the next ODP leg (171A) explored the Barbados accretionary prism, where site 1044 (ODP, 2003) encountered what the Shipboard Party termed a proto-decollement with elevated total gamma-ray emissions from below and the lowest 8–10 m (26–33 ft) of the deformed zone, followed by a fall in gamma rays in the fault zone, with a small peak at the top of the deformed zone. In this respect, site 1044 succession is similar in pattern to our metamorphic case study. Our own examination of logs and seismic data from the Guando field (onshore Colombia; see Leckie et al., 2003, for descriptions) has indicated that similar features occur in faulted oil fields. Our observations may aid those trying to understand the complex and commonly poorly imaged stratigraphy in and below thrust zones.

The deformed succession that does not fit the model is the normal-faulted succession from the Cretaceous of the Crimea. The aspect that marks this fault out is its kinematics and orientation; all other documented examples were shallow or flat-lying zones of deformation such as thrusts, whereas this example is vertical. Nonetheless, some anomalous gamma-ray information was associated with the fault zone, but its character (high K and Th and high Th/K and Th/U ratios) makes it discernable both from flooding surfaces and bedding-parallel deformation. The common observations so far fit best the shallow-dipping structures. To test the applicability of these, a range of other steep and vertical faults have had reconnaissance measurements made during the course of this work (Tables 1–3). These preliminary data suggest that the model does not fit normal and reverse faults but may apply to strike-slip faults. Thrusts and strike-slip fault zones show the most dramatic concentrations of K, U, and sometimes Th. The explanation for this may be that thrusts (and in steeply inclined succession strike-slip faults) concentrate at fine-grained stratigraphic boundaries where elevated levels of K, U, and Th are already present. In other words, the deformed beds may have been hot prior to deformation; now, they are even hotter. Next, we must consider fluid flow. Again, it is the more soluble K and U that are concentrated, suggesting that fluids are important, especially as lubrication of the structure is probably critical, and the existence of fine-grained rock will impede and possibly concentrate fluids. We should also consider volumetrics. At the gross scale, a thrust, slide, or even bedding-parallel zone of fracturing and minor dislocation (stylolite zones) may move a great volume of rock across a possibly wet and fine-grained fault zone. This gives plenty of opportunity for the stripping of K and U (and near certain hosts and acids, Th) and concentration in the fault gouge or mineralized fault. At the smaller scale, the existence of clays and broken minerals in the fault zone provides both the chemistry and surface area for adsorption (Figure 7). Shallow-dipping or flat-lying fault gouge may have the capacity to act as a top seal and thus keep fluids moving against clays below the fault, where K and U may be incorporated. In steep structures, pressure and gravity will propel fluid upward and downward in the fault zone; conversely and the bedding-parallel fault gouge will act as a top seal and spread fluid over a wide area

Table 2. Reverse Faults Measured Using a Spectral Gamma-Ray Device as Background to this Study

Location	Description	TC	K	U	Th	Th/K	Th/U
Lulworth Cove, United Kingdom lat. 2°15′00″, long. 50°38′00″	15-cm (6-in.)-wide calcite-cemented clay gouge; in nonmarine Cretaceous sandstones; undated, probably Paleogene age	15% elevated	5% elevated	10% elevated	not elevated	0.8	0.9
Ballard Cove, United Kingdom lat. 1°56′10″, long. 50°38′00″	reverse fault associated with forced fold; clay gouge, 1.2 m (4 ft) wide in Upper Cretaceous chalk; Paleogene (Alpine) age; accessible by boat	20% elevated	15% elevated	not elevated	10% elevated	0.5	0.7
Ebor, Somerset, United Kingdom lat. 2°41′00″, long. 51°14′00″	strand of the Ebor thrust; weather-back in Carboniferous micritic limestones; Variscan age	10% elevated	no elevation	10% elevated	15% elevated	2	1.2

Table 3. Normal Faults Measured Using a Spectral Gamma-Ray Device as Background to this Study

Location	Description	TC	K	U	Th	Th/K	Th/U
4 km (2.5 mi) east of Thoard, Digne, Alpes de Haute Provence, France lat. 6°10′00″, long. 43°55′00″	1.3-m (4.3-ft)-wide clay fault gouge (northwest-southeast) displaces Oxfordian against Bajocian clays and limestones (Jurassic); detrital clays comprise smectite, illite, and kaolinite; fault gouge is smectite only; probable Paleogene age	20% elevation	0% elevation	10–15% elevation	5% (negligible) elevation	1.5	0.5
Hen Mountain, County Down, northern Ireland lat. 6°8′00″, long. 54°11′00″	17-cm (7-in.)-wide brecciated, kaolinitized zone in Tertiary granite; displacement hard to estimate (over 2 m [6.6 ft]); late Paleogene to Neogene age	25% lower than country rock	20% lower	5–10% lower	negligible	10–20	2–5
Shanklin, Isle of Wight, United Kingdom lat. 1°10′00″, long. 50°37′30″	5–35-cm (2–14-in.)-wide clay gouge (two faults, becoming one at depth) in glauconitic sandstones; 2-m (6.6-ft) vertical displacement; Paleogene to Neogene age	10–15% elevation	10% elevation	0% elevation	5% elevation	0.75	1.5

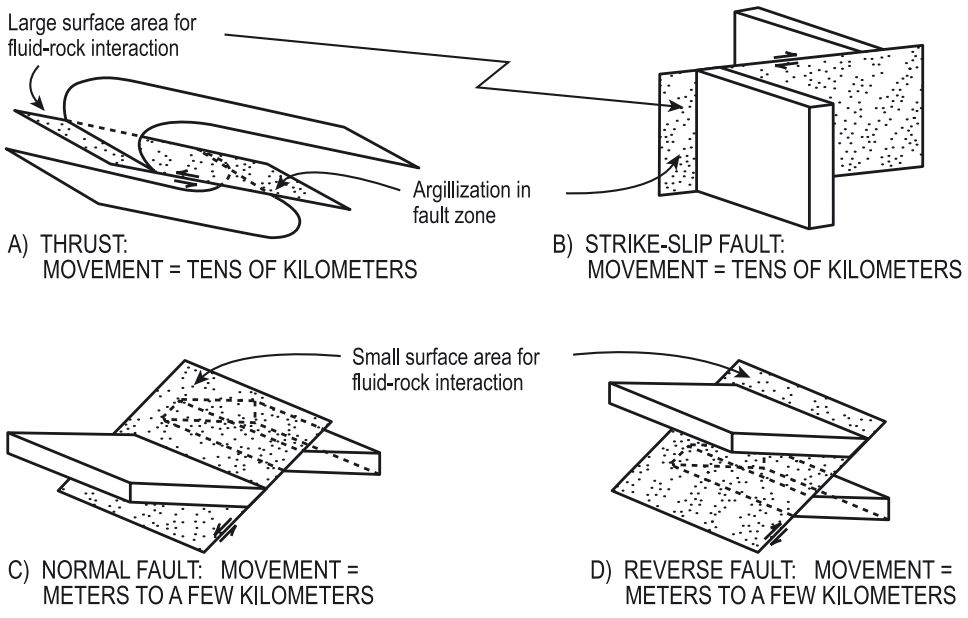

Figure 7. Model showing the possible bedding-fault volumetrics of normal and reverse faults compared to strike-slip and thrusts. The same host rock and fluid composition is assumed. A large area of fine-grained rock is likely to be in the slip surface in thrust faults, allowing a greater surface for argillization and the concentration of K, U, and (sometimes) Th, when incorporated into clays, micas, and other neoformed minerals. In steeply bedded or vertical sedimentary successions adjacent to strike-slip faults, a similar fine-grained bed-to-fault relationship may develop.

(Figure 7). The model is, of course, an oversimplification that does not account for variations in fluid composition, mechanical strength (either side of the fault), or fault geometry. Our model may be tested by two means. In the first test, a comparison of the spectral gamma-ray response across high-angle and low-angle faults of the same age and host rock should produce elevated K and Th and suppressed Th/K and Th/U in the low-angle or bedding-parallel structure. A second test could compare the same bedding-parallel deformed and undeformed flooding surface. Such a common scenario is depicted in idealized form in Figure 8, where the decollement of a listric fault would eventually become bedding parallel and possibly be overlooked during logging. Our model predicts that the hanging-wall decollement will display elevated K and Th and

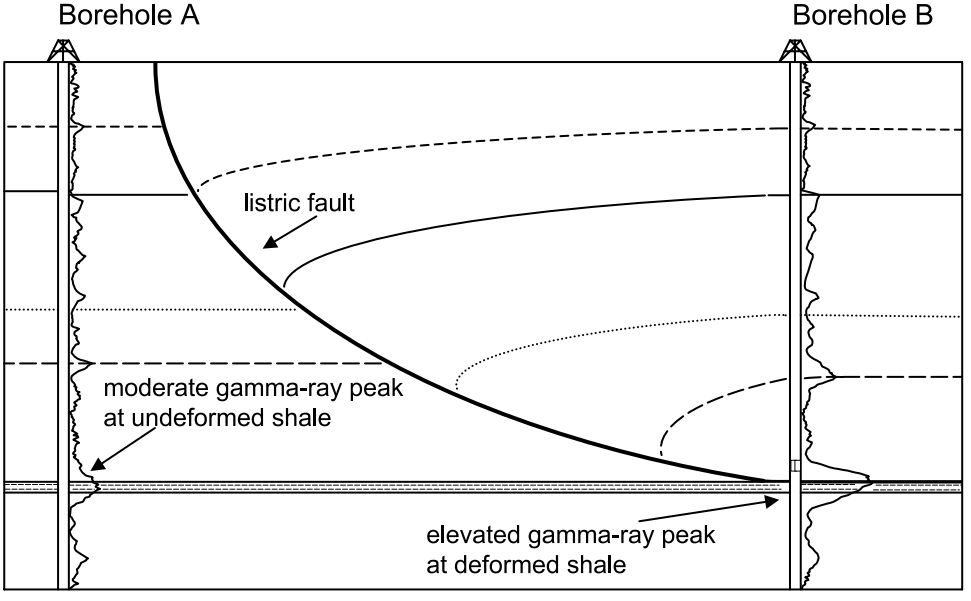

Figure 8. Predicted result of bedding-parallel deformation on a gamma-ray log from an extensional tectonic regime. In this scenario, the shale surface in the hanging-wall succession should show not only the elevated total count gamma-ray radiation but also most likely high K, U, and depressed Th/K and Th/U.

lower Th/K and Th/U but may not be the maximum flooding surface of the sequence. Furthermore, this study has included only limited information from strike-slip faults; this is partly because such structures are less likely to be missed in core or mistaken for stratigraphic surfaces.

CONCLUSIONS

Tectonized outcrops of sedimentary rocks that are weathered or of limited lateral extent and boreholes with or without core may conceal bedding-parallel faults, such as thrusts, slides, and the bases of listric normal faults. Bedding-parallel or stratigraphically restricted fracturing and stylotization may be concentrated in certain beds and likewise remain undetected. Our spectral gamma-ray logs through such fault zones display K, U, Th/K, and Th/U variations akin to flooding surfaces. Bedding-parallel faults may be concentrated at shale partings that formed as flooding surfaces; thus, the fault zone may originally have been hot. The uncommonly large increase in K and U we have detected across fault zones, together with evidence of mineralization above and below the fault zone(s), shows that argillization, mineralization, and fluid flow have accentuated if not caused this spectral gamma-ray response. Four of our case studies show how limited outcrop with dimensions not much larger than borehole core can make spectral gamma-ray–based identification of bedding-parallel zones of tectonism appear like flooding surfaces in channels, on platform limestones, and in a delta succession. In all the bedding-parallel zones of deformation studied, increases in K- and U-based gamma-ray response extended above and below the actual fault gouge. Examination of the rock showed evidence of slickenfibres, stylolites, stretching lineations, and fracturing that increase in intensity with gamma-ray output. This shows that a search of fabric close to bedding-parallel faults can help differentiate a normal flooding surface response from the tectonic response recorded in this work. A normal fault in sandstones (case study from the Crimea) did not display the same flooding surface mimicry in spectral gamma-ray response. Our work on other fault zones and literature review of subsurface examples show that elevated gamma-ray responses from bedding-parallel faults is common. Given similar host rock, fault zone geometry, and fluid composition, thrusts and strike-slip faults are most likely to show elevated K and U, together with Th/K and Th/U, that mimic flooding surfaces (Figure 7). Sedimentary successions above and below horizons, with gamma-ray peaks or low Th/K and Th/U in successions where bedding-parallel faults are possible should be interpreted with caution and examined for associated tectonic fabric.

REFERENCES CITED

Alvaro, M., 1987, La tectonica de cabalgamientos de la Sierra Norte de Mallorca (Islas Baleares): Boletin Geologica y Minieares, v. 98, p. 34–41.

Baraboshkin, E. J., 1999, Berriasian–Valanginian (Early Cretaceous) sea-ways of the Russian platform basin and the problem of Boreal/Tethyan correlation: Geologica Carpathica, v. 50, p. 1–21.

Davies, S. J., and T. Elliott, 1996, Spectral gamma ray characterization of high resolution sequence stratigraphy: Examples from Upper Carboniferous fluvio-deltaic systems, County Clare, Ireland, *in* J. A. Howell and J. F. Aitken, eds., High resolution sequence stratigraphy: Innovations and applications: Geological Society (London) Special Publication 104, p. 25–35.

Dutkiewicz, A., 2001, Hydrocarbon fluid inclusions and pyrobitumen nodules in the uraniferous Matinenda Formation: Implications for oil migration during the early Proterozoic (abs.), *in* F. Noronha, A. Dória, and A. Guedes, eds., XVI ECROFI European Current Research on Fluid Inclusions, Porto 2001: Porto, Portugal, Universidadae do Porto.

Ehrenberg, S. N., and T. A. Svånå, 2000, Use of spectral gamma-ray signature to interpret stratigraphic surfaces in carbonate strata: An example from the Finnmark carbonate platform (Carboniferous–Permian), Barents Sea: AAPG Bulletin, v. 85, no. 2, p. 295–308.

Gelabert, B., F. Sabat, and A. Rodriguez-Perea, 1992, A structural outline of the Serra de Tramuntana of Mallorca (Balearic Islands): Tectonophysics, v. 203, nos. 1–4, p. 167–183.

George, G. T., 2000, Characterisation and high resolution sequence stratigraphy of storm-dominated braid delta and shoreface sequences from the Basal Grit Group (Namurian) of the South Wales Variscan peripheral foreland basin: Marine and Petroleum Geology, v. 17, no. 4, p. 445–475.

Gómez-Graz, D., and A. M. Alonso-Zarza, 2003, Reworked calcretes: Their significance in the reconstruction of alluvial sequences (Permian and Triassic, Minorca, Balearic Islands, Spain): Sedimentary Geology, v. 158, nos. 3–4, p. 299–319.

Gröcke, D. R., G. D. Price, E. Baraboshkin, J. Mutterlose, and A. H. Ruffell, 2003, The Valanginian terrestrial carbon isotope record (abs.): European Union of Geosciences Abstract (EUGXI), Nice, 2003, p. 341.

Hadley, M. J., A. H. Ruffell, and A. G. Leslie, 2000, Gamma-ray spectroscopy in structural correlations: An example from the Neoproterozoic succession of Donegal (NW Ireland): Geological Magazine, v. 137, no. 3, p. 137–152.

Hardenbol, J., P. C. de Graciansky, T. Jacquin, M. B. Farley, and P. R. Vail, 1998, eds., Mesozoic and Cenozoic sequence stratigraphy of western European basins: SEPM Special Publication 42, p. 415–425.

Hurst, A., 1990, Natural gamma-ray spectrometry in hydrocarbon-bearing sandstones from the Norwegian continental shelf, *in* A. Hurst, M. Lovell and A. Morton, eds., Geological applications of wireline logs: Geology Society (London) Special Publication 48, p. 211–222.

Jenkyns, H., B. W. Sellwood, and L. Pomar, 1990, Majorca and the Balearic Islands: London, Geologists' Association, 93 p.

Juodvalkis, A., and K. Barnett, 1997, North Australian Basins Resource Evaluation Workshop Extended Abstracts: Australian Geological Survey Organization Published Record 1997/12, p. 1–12.

Ketzer J. M., S. Morad, R. Evans and I. S Al-Aasm, 2002, Distribution of diagenetic alterations in a sequence stratigraphic framework: Evidence from the Mullaghmore Sandstone Formation (Carboniferous), NW Ireland: Journal of Sedimentary Research, v. 72, no. 6, p. 760–774.

Khryashchevskaya, O., and E. Baraboshkin, 2001, Hauterivian–Barremian sea level fluctuations in central part of northern Caucasus–Scythian platform area (abs.): European Union of Geosciences XI Meeting Abstracts (Strasbourg, France: Symposium EVO7, Geological History of Sea-Water), p. 221.

Kimura, G., E. Silver, P. Blum, P. J. Fox, J. F. Allan, and T. J. G. Francis, 1997, Ocean Drilling Program Leg 170 preliminary report, Costa Rica accretionary wedge: ODP/Texas A&M University, 420 p.

Leckie, D. A., J. M. De Armas, C. Du Toit, K. Glazebrook, E. Gomez, P. Kroshko, B. Norris, A. Parsons, and R. Penas, 2003, Paleogeographic implications of the lower Guadalupe (Dura) Formation in the Guando oil field, Colombia: VIII Simposio Bolivariano— Exploracion Petrolera en las Cuencas Subandinas, Cartegena de Indias, Sept. 21–24, 2003, Memorias: Dublin, Geological Survey of Ireland, v. 2, p. 68–80.

Long, C. B., and B. J. McConnell, 1997, Geology of north Donegal: A geological description to accompany the bedrock geology, North Donegal: Dublin, Geological Survey of Ireland, 1:100,000 scale, sheet 1 and part of sheet 2.

Lucia, F. J., 1999, Carbonate reservoir characterization: Berlin, Springer-Verlag, 226 p.

McRoberts, C. A., H. Furrer, and D. S. Jones, 1998, Palaeoenvironmental interpretation of a Triassic–Jurassic boundary section from Western Australia based on palaeoecological and geochemical data: Palaeogeography, Palaeoclimatology, Palaeoecology, v. 136, p. 79–95.

Millar, G. G., 1990, Fracturing of the northwest Carboniferous basin, Ireland: Ph.D. thesis, The Queen's University of Belfast, Belfast, 350 p.

Ministerio de Industria, 1972, Mapa metalogenetico Palma de Mallorca, Madrid: 44-Madrid-1, Spain, Claudio Coello, Servicio de Publicaciones, 1:2000,000 scale, 1 sheet.

Mitchell, I., and W. Owens, 1994, The Omagh basin, northern Ireland: Geological Magazine, v. 101, p. 99–112.

Myers, K. J., and P. B. Wignall, 1987, Understanding Jurassic organic-rich mudrocks— New concepts using gamma-ray spectrometry and palaeoecology: Examples from the Kimmeridge Clay of Dorset and the Jet Rock of Yorkshire, *in* J. K. Legget and G. G. Zuffa, eds., Marine clastic sedimentology: London, Graham and Trotman, p. 172–189.

Nikishin, A. M., et al., 1998, Scythian platform: Chronostratigraphy and polyphase stages of tectonic history, *in* S. Crasquin-Soleau and E. Barrier, eds., Peri-Tethys Memoir 3: Paris, Memoires Museum Naturelle Histoire et Nature, v. 177, p. 151–162.

Ocean Drilling Program, 2003, ODP Leg 171A logging report: Barbados Accretionary Prism Logging While Drilling: http://www.Ideo.colombia.edu/BRG/ODP/ODP/LEG_SUMM/171A/leg171A.html (accessed May 15, 2003).

Osmond, J. K., and M. Ivanovich, 1992, Uranium-series mobilisation and surface hydrology, *in* M. Ivanovich and R. S. Harmon, eds., Uranium-series disequilibrium: Applications to earth, marine and environmental Sciences: Oxford, Clarendon Press, p. 259–289.

Parkinson, D. N., 1996, Gamma-ray spectrometry as a tool for stratigraphical interpretation: Examples from the western European Lower Jurassic, *in* S. P. Hesselbo and D. N. Parkinson, eds., Sequence stratigraphy in British geology: Geological Society (London) Special Publication 103, p. 231–255.

Price, C., and M. D. Max, 1988, Surface and deep structural control of the NW Carboniferous basin of Ireland: Seismic perspectives of aeromagnetic and surface geological interpretation: Journal of Petroleum Geology, v. 11, no. 4, p. 365–388.

Rosholt, J. N., 1992, Mobilisation and weathering, *in* M. Ivanovich and R. S. Harmon, eds., Uranium-series disequilibrium: Applications to earth, marine and environmental sciences: Oxford, Clarendon Press, p. 167–178.

Ruffell, A., N. Moles, and J. Parnell, 1998, Characterisation and prediction of sediment-hosted ore deposits using sequence stratigraphy: Ore Geology Reviews, v. 12, no. 4, p. 207–223.

Sikka, D. B., 1962, Aero-gamma ray spectrometer aids in the detection of faults: Research Bulletin of the Panjab University, v. 13, parts I–II, p. 91–102.

Slatt, R. M., D. W. Jordan, A. D'Agostino, and R. H. Gillespie, 1992, Outcrop gamma-ray logging to improve understanding of subsurface well log correlations. *in* A. Hurst, C. M. Griffiths, and P. F. Worthington, eds., Geological applications of wireline logs II: Geological Society (London) Special Publication 65, p. 3–19.

Sródon, J., V. A. Drits, D. McCarty, J. C. C. Hsieh, and D. D. Eberl, 2001, Quantitative x-ray diffraction analysis of clay-bearing rocks from random preparations: Clays and Clay Minerals, v. 49, p. 514–528.

Svendsen, J. B., and N. R. Hartley, 2001, Comparison between outcrop-spectral gamma ray logging and whole rock geochemistry: Implications for quantitative reservoir characterisation in continental sequences: Marine and Petroleum Geology, v. 18, no. 6, p. 657–670.

Van Buchem, F. S. P., D. H. Melynk, and I. N. McCave, 1992, Chemical cyclicity and correlation of lower Lias mudstones using gamma-ray logs: Journal of the Geological Society (London), v. 149, p. 991–1002.

Van Wagoner, J. C., R. M. Mitchum, K. M. Campion, and V. D. Rahmanian, 1990, Siliciclastic sequence stratigraphy in well-logs, cores and outcrops: AAPG Methods in Exploration Series 7, 99 p.